

1 **Title: Intestinal infection results in impaired lung innate immunity to**
2 **secondary respiratory infection.**

3 **Subtitle: Lung immunity after gut inflammation.**

4 Shubhanshi Trivedi,¹ Allie H. Grossmann,^{3,5,6} Owen Jensen,¹ Mark J. Cody,⁴ Kristi J.
5 Warren,² Christian C. Yost,^{4,6} and Daniel T. Leung^{1,7}

6 ¹Division of Infectious Disease, ²Division of Pulmonary Medicine, Department of Internal
7 Medicine; ³Huntsman Cancer Institute; ⁴Division of Neonatology, Department of
8 Pediatrics; ⁵Division of Anatomic Pathology, ⁶Molecular Medicine Program; ⁷Division of
9 Microbiology and Immunology, Department of Pathology; University of Utah, Salt Lake
10 City, UT, USA.

11

12

13

14

15

16

17

18

19 **Corresponding author:**

20 Daniel T Leung, M.D.

21 Address: 26 North Medical Drive, Salt Lake City, UT 84132, USA

22 Telephone: 801-581-8804

23 Fax: 801-585-3377

24 Email: daniel.leung@utah.edu

25

26 **Abstract**

27 Pneumonia and diarrhea are among the leading causes of death worldwide, and
28 epidemiological studies have demonstrated that diarrhea is associated with an
29 increased risk of subsequent pneumonia. Our aim was to determine the impact of
30 intestinal infection on innate immune responses in the lung. Using a mouse model of
31 intestinal infection by *Salmonella enterica* serovar Typhimurium (*S. Typhimurium*), we
32 investigated how infection in the gut compartment can modulate immunity in the lungs
33 and impact susceptibility to bacterial (*Klebsiella pneumoniae*) challenge. We found
34 alterations in frequencies of innate immune cells in lungs of intestinally-infected mice
35 compared to uninfected mice. On subsequent challenge with *K. pneumoniae* we found
36 that mice with prior intestinal infection have higher lung bacterial burden and
37 inflammation, increased neutrophil margination, and neutrophil extracellular traps
38 (NETs), but lower overall numbers of neutrophils, compared to mice without prior
39 intestinal infection. Together, these results suggest that intestinal infection impacts lung
40 innate immune responses, most notably neutrophil characteristics, potentially resulting
41 in increased susceptibility to secondary pneumonia.

42

43

44

45

46

47

48 **Author summary**

49 Infections of the lung and gut are among the leading causes of death worldwide. Human
50 studies have shown that children with diarrhea are at higher risk of subsequent lung
51 infection. How intestinal infections impact lung immunity is not well known. In the
52 present study, we reveal that bacterial infection of the intestinal mucosa may
53 compromise lung immunity, offering new insights into increased susceptibility to
54 respiratory infections. We found that upon respiratory infection, mice with prior intestinal
55 infection are more moribund and despite having higher bacterial burden, they show
56 reduced numbers of neutrophils in the lung compared to mice without prior intestinal
57 infection. We also found excessive neutrophil extracellular traps formation in the lungs
58 of mice with prior intestinal infection, providing evidence of increased pulmonary tissue
59 damage. Collectively, these data identify a direct link between pulmonary and enteric
60 infection and suggests gut infections impair neutrophils responses in the lungs.

61 Introduction

62 Diarrhea and pneumonia are among the leading causes of death worldwide. In children
63 alone, these diseases combine to kill ~1.4 million each year, with the majority of these
64 deaths occurring in lower and middle-income countries [1]. Epidemiological studies
65 have shown that children are at an increased risk of pneumonia following a diarrheal
66 episode [2-5]. However, the immunological mechanisms behind an increased
67 susceptibility to such secondary respiratory infections are not well understood.

68 Although the gastrointestinal and respiratory tracts have different environments and
69 functions, there is emerging data showing cross-talk between these two mucosal sites
70 in chronic inflammatory diseases such as inflammatory bowel disease (IBD), asthma,
71 and chronic obstructive pulmonary disease [6-10]. Additionally, there is emerging
72 evidence that the intestinal microbiota plays a role in host defense against bacterial
73 pneumonia [11, 12]. The gastrointestinal and respiratory tracts share the same
74 embryonic origin and have common components of the mucosal immune system such
75 as an epithelial barrier, submucosal lymphoid tissue, the production of IgA and
76 defensins, toll-like receptor expression, and the presence of innate lymphocytes and
77 dendritic cells [13]. Leukocytes circulate between peripheral tissue, lymphatics, and
78 blood, to survey for foreign antigens. Notably, several innate-like leukocytes, such as
79 Mucosal Associated Invariant T (MAIT) cells, invariant Natural Killer T (iNKT) cells,
80 gamma delta T ($\gamma\delta$ T) cells, innate lymphoid cells (ILCs), dendritic cells (DC) and
81 neutrophils, have the capacity to circulate between tissues, and play important roles in
82 both respiratory and intestinal tract immunity [14-17].

83 It is anticipated that organs with the same embryonic origin share the same pathological
84 specificities in a disease, for example, an increased number of inflammatory cells have
85 been reported in bronchoalveolar lavage (BAL) fluid [18] and sputum [19] of IBD
86 patients. How intestinal infection impacts immunity in the lung is not known. In this
87 study, we examine the impact of intestinal infection on the immune response in the
88 lungs of mice using *Salmonella enterica* serovar Typhimurium (*S. Typhimurium*), an
89 established model of intestinal infections. We found that mice infected with *S.*
90 *Typhimurium* have increased susceptibility to respiratory *Klebsiella pneumoniae*

91 infection compared to mice without prior intestinal infection. Prior intestinal infection
92 modulated effector cells of innate immunity in the lung, contributing to respiratory
93 immune dysregulation and a higher *K. pneumoniae* bacterial burden. This study furthers
94 our understanding of the gut-lung immunological crosstalk, and begins to define the
95 mechanisms of increased susceptibility to secondary pneumonia following diarrheal
96 infections.

97 **Results**

98 **1. Mice with prior *S. Typhimurium* intestinal infection have increased lung** 99 **bacterial load, sickness score, and susceptibility to respiratory *K. pneumoniae*** 100 **infection.**

101 To test whether prior intestinal infection increases the susceptibility to respiratory *K.*
102 *pneumoniae* infection, we evaluated survival, body weight loss, sickness score, and
103 bacterial burden in lungs post *K. pneumoniae* challenge. Compared to *S. Typhimurium*
104 infected mice, which had a survival rate of 90-100%, and *K. pneumoniae* infected mice,
105 which had a survival of 60-80%, mice with prior *S. Typhimurium* intestinal infection had
106 a survival rate of 0-30% at 120 hours post *K. pneumoniae* infection (Fig 1A).

107 Interestingly, although there were no statistically significant differences in body weight
108 loss between mice with or without *S. Typhimurium* infection with *K. pneumoniae*
109 challenge (Supplementary Figure S1), mice with prior intestinal infection had a higher
110 sickness score (Fig 1B). This sickness scoring system included hunched posture, ruffled
111 fur, decreased movement and altered respiratory rates and quality of breaths (Fig 1C).
112 Of note, mice with only *S. Typhimurium* intestinal infection showed no weight loss and
113 had reduced sickness scores. When bacterial burden was evaluated at 18 and 33 hours
114 post *K. pneumoniae* infection, we found significantly higher lung bacterial burden in
115 mice with prior intestinal infection compared to mice without prior intestinal infection (Fig
116 1D and 1E). We did not find any *S. Typhimurium* bacterial burden in lungs of mice with
117 intestinal infection.

118

119 **2. Mice with prior *S. Typhimurium* intestinal infection have increased lung** 120 **inflammation from subsequent respiratory *K. pneumoniae* infection.**

121 We next examined the degree of lung inflammation by histological analysis of tissue
122 sections from all four groups of mice. Histopathological analysis revealed mixed
123 interstitial inflammatory consolidations in mice with *K. pneumoniae* respiratory infection
124 and increased microabscess formation with pyknotic neutrophils in mice co-infected with
125 *S. Typhimurium* and *K. pneumoniae* (Fig 2A). Uninfected mice and mice with intestinal
126 infection showed normal alveolar and interstitial lung histology (Fig 2A). Upon challenge
127 with *K. pneumoniae* respiratory infection, mice with prior *S. Typhimurium* intestinal

128 infection also showed marked intravascular clustering of polymorphonuclear neutrophils
129 (PMNs), with increased margination, necrotic cluster formation and extravasation (Fig
130 2B and Supplementary Figure S2). Intravascular neutrophil clustering was noticeably
131 absent in the other treatment groups. Furthermore, lung sections from mice with
132 intestinal infection, and mice with both intestinal and respiratory infection, showed
133 scattered microthrombi in capillary-sized vessels whereas mice with *K. pneumoniae*
134 respiratory infection (with no prior intestinal infection) showed no microthrombi formation
135 (Supplementary Figure S3).

136

137 **3. Mice with prior *S. Typhimurium* intestinal infection have altered lung cytokine** 138 **profiles after *K. pneumoniae* challenge.**

139 The delicate balance between pro- and anti-inflammatory cytokines is crucial in
140 containing pathogens and maintaining tissue repair and homeostasis in the lung [11].
141 Prior studies have shown the importance of cytokines such as IFN- γ in recruitment of
142 neutrophils to the lung tissue [20, 21]. We investigated whether intestinal infection
143 affected cytokine production in lung homogenates, and whether prior intestinal infection
144 affected this cytokine response to intranasal *K. pneumoniae* challenge. Our results
145 indicate that compared with the uninfected control group, *S. Typhimurium* infected mice
146 had significantly higher lung levels of IFN- γ , MCP-1 and IL-1 β (Fig 3 A,B and C). While
147 Thy1-expressing natural killer (NK) cells [22] and NKp46⁺ ILC3 [23] cells are commonly
148 thought as the sources of IFN- γ , there is a mounting evidence that neutrophils are a
149 prominent cellular source of IFN- γ during the innate phase of *S. Typhimurium*-induced
150 colitis [24]. It is possible that large number of primed neutrophils traffick to lungs after
151 intestinal infection, contribute to cytokine production and increases the potential for
152 neutrophil-mediated pathology or NET formation upon secondary infection [17].
153 Furthermore, following *K. pneumoniae* challenge, mice with prior intestinal infection had
154 higher levels of IFN- γ and lower levels of GM-CSF cytokine production in lung
155 homogenates compared to those without prior intestinal infection (Fig 3A and D). Levels
156 of IL-23, IL-1 α , TNF α , IL-12p70, IL-10, IL-6, IL-27, IL-17A and IFN- β were not
157 significantly different between mice with and without prior intestinal infection
158 (Supplementary Figure S4).

159 **4. Mice with prior *S. Typhimurium* intestinal infection have lower number of**
160 **neutrophils in lung after *K. pneumoniae* challenge.**

161 We next examined the impact of intestinal infection on innate cellular responses in the
162 lung, and also its effect on such responses to *K. pneumoniae* respiratory challenge. We
163 analyzed changes in major innate lung leukocytes (plasmacytoid dendritic cells (pDCs),
164 monocyte-derived dendritic cells (moDCs), CD103⁺ DCs, neutrophils, alveolar
165 macrophages (AMs) and interstitial macrophages (IMs)) pre- and post-*K. pneumoniae*
166 challenge in mice infected with *S. Typhimurium*. Consistent with previous studies [9], we
167 observed rapid and robust recruitment of neutrophils to the lungs at 18 hours following
168 *K. pneumoniae* infection compared to uninfected controls. Interestingly, mice with prior
169 intestinal infection had significantly lower frequencies and total number of lung
170 neutrophils following *K. pneumoniae* challenge compared to *K. pneumoniae* infected
171 mice (Fig 4A and Supplementary Figure 5A). Furthermore, results indicated that
172 frequencies of pDCs increased and moDCs decreased in the lungs of *S. Typhimurium*
173 intestinally infected mice compared to uninfected controls (Fig 4B and C). Following
174 intranasal *Klebsiella* challenge, we found a marked increase in frequencies of pDCs and
175 significantly lower frequencies of moDCs in mice with prior intestinal infection compared
176 to those without prior intestinal infection (Fig 4B and C). No significant differences were
177 observed in frequencies of CD103⁺ DCs (Fig 4D), AMs and IMs (Fig 4E and F) between
178 *K. pneumoniae* infected mice with and without prior intestinal infection. Total numbers of
179 pDCs, moDCs, CD103⁺ DCs, AMs or IMs were not different in mice with prior intestinal
180 infection compared to those without prior intestinal infection (Supplementary Figure S5
181 B-F). We also found higher numbers of neutrophils, pDCs and IMs and lower numbers
182 of CD103⁺ DCs in mice with only intestinal infection compared to uninfected mice
183 (Supplementary Figure S5 B-F).

184
185 We also investigated innate-like T cells including mucosal-associated invariant T (MAIT)
186 cells, invariant natural killer T (iNKT) cells and $\gamma\delta$ T cells as they are known to play an
187 important role in bacterial infections [10]. No differences were observed in percentage
188 frequencies of iNKT cells, MAITs or $\gamma\delta$ T cells between mice with and without prior
189 intestinal infection (Supplementary Figure S6). Furthermore, when complete blood

190 counts were assessed with a Hemavet analyzer, no significant differences were
191 observed in circulating neutrophils, lymphocytes, monocytes, eosinophils, basophils and
192 platelets between mice with and without prior intestinal infection (Supplementary Figure
193 S7).

194

195 **5. Mice with prior *S. Typhimurium* intestinal infection induces widespread** 196 **NETosis after *K. pneumoniae* challenge.**

197 Recent studies have revealed that excessive NET formation plays a role in pathogen-
198 associated lung injury, including in models of bacterial pneumonia [25-28]. Our
199 histopathological analysis revealed clusters of pyknotic neutrophils and thrombus
200 formation in mice with prior intestinal infection (Fig 2 and Supplementary figure 3). It is
201 known that neutrophils constitute the main cellular component of thrombi, and mainly
202 participate in thrombosis by releasing NETs [29]. Moreover, we detected higher levels of
203 IFN- γ in mice with prior intestinal infection compared to mice without prior intestinal
204 infection (Fig 3), and IFN- γ can promote NET formation by neutrophils [30]. We
205 therefore explored whether prior intestinal infection induces NET formation. We
206 examined citrullinated histones and myeloperoxidase (MPO) in lung tissues of each
207 experimental group by immunofluorescence. As expected, significantly higher number
208 of NETs ($p = 0.0006$) were detected in mice with prior intestinal infection compared to
209 those without prior intestinal infection (Fig 5 A and B), as demonstrated by the presence
210 of extracellular DNA overlaid with citrullinated histone 3 and MPO (Fig 5A). Mock-
211 infected lungs did not show any staining for citrullinated histone 3 or MPO (Fig 5A). We
212 detected NETs in lung tissues of mice with *S. Typhimurium* intestinal infection
213 compared to uninfected control or *K. pneumoniae* infected alone, and there was no
214 significant difference between these groups (Fig 5B).

215 Discussion

216 We found that bacterial intestinal infection in mice adversely impacts immunity in the
217 lung, increasing susceptibility to secondary respiratory infection. We show that mice
218 with prior intestinal *S. Typhimurium* infection have higher lung bacterial burden and
219 sickness scores after subsequent *K. pneumoniae* challenge compared to mice without
220 prior *S. Typhimurium* infection. This finding was associated with changes in innate
221 cellular responses, most notably those of neutrophils, which were decreased in the
222 parenchyma, clustering in the lung vasculature, and associated with increased NETosis
223 in those with secondary infection. As neutrophils are essential for pulmonary clearance
224 of bacterial infections such as *K. pneumoniae* [31], it is possible that intestinal infection
225 impairs the recruitment and function of lung neutrophil responses against *K.*
226 *pneumoniae*, leading to an inability to clear the lung bacterial infection, thereby
227 worsening airway disease.

228

229 In addition to epidemiological studies showing a higher susceptibility to pulmonary
230 infections after intestinal infection in children [2-5], and that intestinal diseases are often
231 associated with pulmonary disorders [32-34], the immunological crosstalk of the lung-
232 gut axis is not well understood. In the context of IBD, it has been proposed that
233 intestinal inflammation and increased cytokine levels create conditions favorable for
234 neutrophil margination onto the lung endothelium [35, 36]. When the lung encounters a
235 secondary insult, neutrophil recruitment, activation and extravasation could mediate
236 lung tissue injury and IBD-induced respiratory diseases [17, 37]. Our knowledge of how
237 intestinal infection impacts the recruitment, extravasation and function of neutrophils in
238 tissues outside of the intestine is limited. Studies have shown that GM-CSF plays an
239 important role in neutrophil accumulation [38, 39], and GM-CSF is protective in
240 preclinical models of pneumonia-associated lung injury [40, 41]. We found a significantly
241 lower lung GM-CSF response to *K. pneumoniae* infection in mice with prior intestinal
242 infection, which may decrease the lung's ability to recruit circulating neutrophils,
243 resulting in an increased susceptibility to infection. In line with this, we also detected
244 increased NETosis and microthrombosis in *K. pneumoniae* infection in mice with prior

245 intestinal infection as compared to mice without prior intestinal infection. It is likely that
246 NETs and NET-associated factors, including histones and granule proteases, mediate
247 vascular and tissue injury and contribute to microthrombosis [42-45]. The activation of
248 NETosis also causes changes in neutrophil morphology including cell membrane
249 rupture and neutrophil death [46]. We speculate that prior intestinal infection induces
250 suicidal NETosis contributing to lower numbers of viable neutrophils in lungs. Future
251 studies examining the mechanisms governing neutrophil activity, and activation of
252 NETosis, in lung after intestinal infection are warranted.

253

254 Nonconventional T lymphocytes including MAIT cells, \mathbb{N} KT cells and $\gamma\delta$ -T cells, have
255 tissue-homing properties, and have been implicated in protection against respiratory
256 bacterial infections [15]. Here, we found no differences in frequencies or number of
257 these cells between the groups tested. Likewise, except for IFN- γ we did not find any
258 differences in cytokines that have been implicated in lung defense against bacterial
259 pathogens, including IL-17A [47], TNF- α [48] and IL-10 [49, 50]. Both a protective [51]
260 and detrimental [52] role of IFN- γ has been reported against bacterial infections, and we
261 found significant increase in lung IFN- γ production in mice with intestinal infection. The
262 importance of IFN- γ production in our model is unclear and merits investigation. We
263 observed higher frequencies of pDCs in lungs of mice with prior intestinal infection, and
264 this may be related to the role of respiratory pDCs in tissue repair [53]. Alternatively,
265 accumulation of pDCs in lung post intestinal infection may have involvement in the
266 initiation of inflammation and antigen-specific T cell responses [54]. Moreover,
267 frequencies of moDCs, which may contribute to control of secondary respiratory
268 infection, was decreased in mice with prior intestinal infection [55, 56].

269

270 Our study has several limitations. Firstly, we did not account for the effect of the pre-
271 existing intestinal microbiota; however, all mice were purchased from the same source,
272 and were cohoused prior to infection. Secondly, we did not evaluate serum levels of IL-
273 6, TNF- α , IFN- γ and VEGF [35, 36] and neutrophil chemokines such as keratinocyte-
274 derived chemokine (KC) [57], macrophage inflammatory protein 2 (MIP-2) [58], CXC

275 receptor 2 (CXCR2) and CXC ligand 5 (CXCL5) [59] which would further our
276 understanding of lung neutrophil trafficking following intestinal inflammation. Lastly, we
277 have not investigated the role of innate lymphoid cells, which have shown to be
278 recruited from gut to the lungs in response to inflammation [60, 61] [62].

279

280 In conclusion, the present study demonstrates that infection in the gut adversely
281 impacts immunity in the lung and reveals potential mechanisms of immunological
282 crosstalk between the lung and gut during enteric infection. While epidemiological
283 studies have demonstrated this lung-gut association, we provide here novel findings
284 that intestinal infection modulates neutrophil and cytokine responses in the lung,
285 resulting in an increased susceptibility to a secondary pneumonia challenge. These data
286 have the potential to inform efforts to prevent and treat respiratory infections in those
287 with intestinal infection or inflammation.

288 **Materials and Methods**

289 **Bacterial strains**

290 *Salmonella enterica* serovar Typhimurium (provided by Dr. June Round) was grown
291 overnight in Luria Broth (LB) supplemented with 100 µg/ml ampicillin and *K.*
292 *pneumoniae* (subsp. *pneumoniae* (Schroeter) Trevisan (ATCC® 43816™), serotype 2)
293 was grown overnight in Tryptic Soy Broth (TSB) at 37°C in a shaking incubator.
294 Overnight cultures were diluted 1:10 in fresh medium and sub-cultured for 4 h under
295 mild aeration. Bacteria were washed twice in phosphate-buffered saline (PBS) and then
296 suspended in 1 ml PBS. *S.* Typhimurium culture (OD₆₀₀ = 0.1) was further diluted 1:10⁴
297 in PBS and given to mice in 100 µl volume. *K. pneumoniae* (OD₆₀₀ = 0.4) culture was
298 further diluted 1:10 and given to mice in 50 µl volume. Bacterial colony forming units
299 (CFUs) were confirmed by culturing on LB + ampicillin agar plates for *S.* Typhimurium
300 and MacConkey agar plates for *K. pneumoniae*.

301

302 **Mice and inoculations**

303 Six to eight week old female C57BL/6J wild type mice were obtained from Jackson
304 Laboratories. All animals were maintained and experiments were performed in
305 accordance with University of Utah and Institutional Animal Care and Use Committee
306 (IACUC) approved guidelines (protocol no. 17-01011). The animals were kept at a
307 constant temperature (25°C) with unlimited access to pellet diet and water in a room
308 with a 12 h light/dark cycle. All animals were monitored daily and infected animals were
309 scored for the signs of clinical illness severity [63]. Animals were ethically euthanized
310 using CO₂.

311

312 For the experiments, all mice were pretreated with streptomycin as described previously
313 [64]. Briefly, water and food were withdrawn 4 hours before oral gavage treatment with
314 7.5 mg of streptomycin in 100 µl HBSS. Afterward, animals were supplied with water
315 and food ad libitum. At 20 h after streptomycin treatment, water and food were
316 withdrawn again for 4 hours before the mice were infected with 10⁴ CFU of serovar
317 Typhimurium (oral gavage of 100 µl suspension in PBS) or treated with sterile PBS
318 (control). (Note: we selected this dose of *S.* Typhimurium based on titration experiments

319 showing that at this dose, bacteria could be cultured from stool but not from lungs).
320 Thereafter, drinking water and food ad libitum was offered immediately. Six days post
321 infection (p.i.), mice were sacrificed by CO₂ asphyxiation, and lungs were removed for
322 analysis.

323

324 For *K. pneumoniae* challenge experiments, six days post *S. Typhimurium* infection,
325 isoflurane anesthetized mice were inoculated intranasally with ~ 10¹⁰ CFU *K.*
326 *pneumoniae* in 50 µl volume. Inoculated mice were observed until fully recovered from
327 anesthesia and euthanized at 18 h post infection for *K. pneumoniae* bacterial load
328 enumeration and innate immune response assessment. For survival studies, to reduce
329 animal pain and respiratory distress, *K. pneumoniae* dose was reduced to 10⁵ CFU .

330

331 **Lung Histology**

332 After sacrifice, mouse lungs were infused with 10% neutral buffered formalin via the
333 trachea, fixed in formalin overnight, dehydrated in 70% ethyl alcohol and embedded in
334 paraffin. 4 µm sections were stained with haematoxylin and eosin (H&E) and analysed
335 by a board certified anatomic pathologist (A.H.G.). Samples were blinded prior to
336 histopathologic analysis.

337

338 **Lung Neutrophil Extracellular Trap Assessment**

339 Paraffin imbedded mouse lung were cut at 8 µm thickness on a microtome. Sections
340 were deparaffinized and rehydrated following xylene and decreasing concentration of
341 ethanol washes. Heat induced epitope antigen retrieval of lung sections were
342 processed in a 2100 Retriever Thermal Processor (Electron Microscopy Sciences,
343 210050) containing Citrate buffer pH 6.0 solution (abcam, ab93678). Sections were
344 incubated for 10 minutes with 0.1% Triton-X-100 and blocked with 10% Donkey Serum
345 for 1 hour at RT. Antibodies for citrullinated Histone H3 (Abcam, ab5103) and
346 Myeloperoxidase (R&D Systems, AF3667) were incubated at 1:100 dilution in 10%
347 donkey serum overnight at 4°C. After washing sections with PBS, secondary rabbit and
348 goat antibodies conjugated to Alexa Fluor 488 or Alexa Fluor 546, respectively, along
349 with DAPI nuclear stain were incubated on sections for 90 minutes at 4°C. Sections

350 were washed and coverslips were adhered with aqueous mounting medium (Dako,
351 S3025). Images were acquired on an Olympus FV3000 Confocal Laser Scanning
352 Microscope at 20X and 60X magnification. FluoView software (Olympus) and ImageJ
353 Fiji (NIH) were used for image processing and analysis. We quantified NET formation
354 on the images using a standardized grid system as previously described [65]. Briefly,
355 we used ImageJ software to place a standardized grid on randomly selected high-power
356 field images (n=5 field images/sample). The number of times that any NET crossed a
357 grid line was tallied.

358

359 **Lung mononuclear cell isolation**

360 For lung digestion and preparation of single cell suspensions, lungs were perfused
361 using 5 mL sterile PBS, aseptically harvested from euthanized mice and kept in RPMI
362 with 10% Fetal Bovine Serum (FBS). Lungs were dissociated using the mouse Lung
363 Dissociation Kit (Miltenyi Biotec) and the gentleMACS Dissociator (Miltenyi Biotec) as
364 per manufacturer's instructions. After dissociation, cells were passed through a 70 μ m
365 cell strainer and washed with RPMI with 10% FBS. Red blood cells were lysed with red
366 blood cell lysis buffer. Lung mononuclear cells were then washed twice in RPMI with
367 10% FBS before use in subsequent experiments.

368

369 **Bacterial Load quantification**

370 *K. pneumoniae* bacterial load was determined by plating ten-fold serial dilutions of the
371 lung homogenates onto MacConkey agar plates (Sigma-Aldrich). The plates were
372 incubated at 37°C overnight before bacterial CFUs were determined by colony counts.

373

374 **Mouse inflammation quantification**

375 Lungs homogenates were filtered on 70 μ m cell strainers and centrifuged at 300 \times g for
376 5 min. Supernatants were stored at -80°C for cytokine content analysis. Lung cytokine
377 levels were assessed from the supernatant samples via LEGENDplex kit (mouse
378 inflammation panel 13-plex; BioLegend) per manufacturer's instructions. Cytokine levels
379 were acquired using a FACSCanto II flow cytometer (BD Biosciences, San Jose, CA),
380 and analyses were performed using LEGENDplex data analysis software (BioLegend).

381 **Tetramer and antibody surface-staining of lung single cell suspensions**

382 From each group of animals, 1-2 million cell aliquots were prepared and stained with the
383 fixable viability dye eFluor™ 780 (eBioscience) for 15 min at room temperature (RT) to
384 exclude dead cells from analysis. The cells were washed with PBS + 2% FBS and
385 incubated with anti-mouse CD16/CD32 Fc Block antibody (BD Biosciences, USA), for
386 20 min at 4 °C. Cells were then stained for 30 min at RT with appropriately diluted PE
387 conjugated MR-1-5-OP-RU tetramers or α -GalCer (PBS-44)-loaded CD1d tetramer
388 conjugated to APC, anti-CD3-FITC (Biolegend), anti-CD161-BV510 (Biolegend), anti-
389 CD49b-BV711 (BD), anti-TCR $\gamma\delta$ -PE-Cy7 (Biolegend), anti-TCR β -BV421 (Biolegend),
390 anti-CD45R-PE-Cy5 and anti-CD44-BV650 (Biolegend). To evaluate different antigen
391 presenting cells, after Fc Block incubation, cells were also surface stained with anti-
392 CD45 AF700 (Biolegend), anti-CD11b-FITC (Biolegend), anti-CD11c-PE Cy-7 (BD),
393 anti-Siglec-F- BV711 (BD), anti-CD64-BV605 (Biolegend), anti-CD24-PE (Biolegend),
394 anti-Ly-6G-PerCP-Cy5.5 (Biolegend), anti-CD103-BV510 (Biolegend), anti-mPDCA-1
395 APC (Miltenyi Biotec) and anti-MHC II BV421 (Biolegend) for 30 min at 4 °C. A total of
396 10^6 gated events per sample were collected using the BD Fortessa flow cytometer
397 (Becton Dickinson, San Diego, CA), and results were analyzed using FlowJo 10.4.2
398 software.

399

400 **Statistical analysis**

401 GraphPad Prism 6 software was used for statistical analysis. The Mann-Whitney *U* test
402 was used for comparison of continuous variables between uninfected and *S.*
403 *Typhimurium* infected group and between mice with prior intestinal infection and without
404 prior intestinal infection. Results were presented as mean \pm standard deviation, and $p <$
405 0.05 was considered statistically significant.

406

407 **Acknowledgements**

408 This work was supported in part by grant W81XWH-17-1-0109 from the Department of
409 Defense (to D.T.L.), and by the National Institutes of Health (R01 HD093826 to C.C.Y.).
410 This work was supported by the University of Utah Flow Cytometry Facility in addition to

411 the National Cancer Institute through Award Number 5P30CA042014-24, and CMC
412 animal facility. We would also like to thank Cole Anderson, Michael Graves, Alexandra
413 Heitkamp and Melanie Prettyman for their technical assistance.

414 **References**

- 415 1. Liu L, Oza S, Hogan D, Chu Y, Perin J, Zhu J, et al. Global, regional, and national
416 causes of under-5 mortality in 2000–15: an updated systematic analysis with
417 implications for the Sustainable Development Goals. *The Lancet*.
418 2016;388(10063):3027-35. doi: 10.1016/s0140-6736(16)31593-8.
- 419 2. Ashraf S, Huque MH, Kenah E, Agboatwalla M, Luby SP. Effect of recent diarrhoeal
420 episodes on risk of pneumonia in children under the age of 5 years in Karachi, Pakistan.
421 *International Journal of Epidemiology*. 2013;42(1):194-200. doi: 10.1093/ije/dys233.
- 422 3. Leung DT, Das SK, Faruque ASG, Malek MA, Chisti MJ, Qadri F, et al. Concurrent
423 Pneumonia in Children Under 5 Years of Age Presenting to a Diarrheal Hospital in
424 Dhaka, Bangladesh. *The American Journal of Tropical Medicine and Hygiene*.
425 2015;93(4):831-5. doi: 10.4269/ajtmh.15-0074.
- 426 4. Schmidt WP, Cairncross S, Barreto ML, Clasen T, Genser B. Recent diarrhoeal
427 illness and risk of lower respiratory infections in children under the age of 5 years.
428 2009;38(3):766-72. doi: 10.1093/ije/dyp159.
- 429 5. Walker CL, Perin J, Katz J, Tielsch JM, Black RE. Diarrhea as a risk factor for acute
430 lower respiratory tract infections among young children in low income settings. *J Glob
431 Health*. 2013;3(1):010402. Epub 2013/07/05. doi: 10.7189/jogh.03.010402. PubMed
432 PMID: 23826506; PubMed Central PMCID: PMC3700029.
- 433 6. Liu Y, Wang X-Y, Yang X, Jing S, Zhu L, Gao S-H. Lung and Intestine: A Specific
434 Link in an Ulcerative Colitis Rat Model. 2013;2013:1-13. doi: 10.1155/2013/124530.
- 435 7. Powell N, Walker MM, Talley NJ. Gastrointestinal eosinophils in health, disease and
436 functional disorders. *Nat Rev Gastroenterol Hepatol*. 2010;7(3):146-56. Epub
437 2010/02/04. doi: 10.1038/nrgastro.2010.5. PubMed PMID: 20125092.
- 438 8. Rutten EPA, Lenaerts K, Buurman WA, Wouters EFM. Disturbed intestinal integrity
439 in patients with COPD: effects of activities of daily living. *Chest*. 2014;145(2):245-52.
440 Epub 2013/08/10. doi: 10.1378/chest.13-0584. PubMed PMID: 23928850.
- 441 9. Tulic MK, Piche T, Verhasselt V. Lung-gut cross-talk: evidence, mechanisms and
442 implications for the mucosal inflammatory diseases. *Clinical & Experimental Allergy*.
443 2016;46(4):519-28. doi: 10.1111/cea.12723.

- 444 10. Wang H, Liu J-S, Peng S-H, Deng X-Y, Zhu D-M, Javidiparsijani S, et al. Gut-lung
445 crosstalk in pulmonary involvement with inflammatory bowel diseases. *World J*
446 *Gastroenterol.* 2013;19(40):6794-804. Epub 2013/10/28. doi: 10.3748/wjg.v19.i40.6794.
447 PubMed PMID: 24187454.
- 448 11. Schuijt TJ, Lankelma JM, Scicluna BP, De Sousa E Melo F, Roelofs JJTH, De Boer
449 JD, et al. The gut microbiota plays a protective role in the host defence against
450 pneumococcal pneumonia. *Gut.* 2016;65(4):575-83. doi: 10.1136/gutjnl-2015-309728.
- 451 12. Tsay T-B, Yang M-C, Chen P-H, Hsu C-M, Chen L-W. Gut flora enhance bacterial
452 clearance in lung through toll-like receptors 4. 2011;18(1):68. doi: 10.1186/1423-0127-
453 18-68.
- 454 13. Budden KF, Gellatly SL, Wood DLA, Cooper MA, Morrison M, Hugenholtz P, et al.
455 Emerging pathogenic links between microbiota and the gut–lung axis. *Nature Reviews*
456 *Microbiology.* 2017;15(1):55-63. doi: 10.1038/nrmicro.2016.142.
- 457 14. Bennett MS, Round JL, Leung DT. Innate-like lymphocytes in intestinal infections.
458 *Current Opinion in Infectious Diseases.* 2015;28(5):457-63. doi:
459 10.1097/qco.0000000000000189.
- 460 15. Ivanov S, Paget C, Trottein F. Role of Non-conventional T Lymphocytes in
461 *Respiratory Infections: The Case of the Pneumococcus.* 2014;10(10):e1004300. doi:
462 10.1371/journal.ppat.1004300.
- 463 16. Ruane D, Brane L, Reis BS, Cheong C, Poles J, Do Y, et al. Lung dendritic cells
464 induce migration of protective T cells to the gastrointestinal tract. *J Exp Med.*
465 2013;210(9):1871-88. Epub 2013/08/21. doi: 10.1084/jem.20122762. PubMed PMID:
466 23960190; PubMed Central PMCID: PMC3754860.
- 467 17. Mateer SW, Maltby S, Marks E, Foster PS, Horvat JC, Hansbro PM, et al. Potential
468 mechanisms regulating pulmonary pathology in inflammatory bowel disease.
469 2015;98(5):727-37. doi: 10.1189/jlb.3ru1114-563r.
- 470 18. Bonniere P, Wallaert B, Cortot A, Marchandise X, Riou Y, Tonnel AB, et al. Latent
471 pulmonary involvement in Crohn's disease: biological, functional, bronchoalveolar
472 lavage and scintigraphic studies. 1986;27(8):919-25. doi: 10.1136/gut.27.8.919.
- 473 19. Fireman Z, Osipov A, Kivity S, Kopelman Y, Sternberg A, Lazarov E, et al. The use
474 of induced sputum in the assessment of pulmonary involvement in Crohn's disease. *Am*

- 475 J Gastroenterol. 2000;95(3):730-4. Epub 2000/03/10. doi: 10.1111/j.1572-
476 0241.2000.01843.x. PubMed PMID: 10710066.
- 477 20. Yamada M, Gomez JC, Chugh PE, Lowell CA, Dinauer MC, Dittmer DP, et al.
478 Interferon- γ production by neutrophils during bacterial pneumonia in mice. American
479 journal of respiratory and critical care medicine. 2011;183(10):1391-401. Epub
480 2010/12/17. doi: 10.1164/rccm.201004-0592OC. PubMed PMID: 21169470.
- 481 21. Pechous RD. With Friends Like These: The Complex Role of Neutrophils in the
482 Progression of Severe Pneumonia. Front Cell Infect Microbiol. 2017;7:160-. doi:
483 10.3389/fcimb.2017.00160. PubMed PMID: 28507954.
- 484 22. Kupz A, Scott TA, Belz GT, Andrews DM, Greyer M, Lew AM, et al. Contribution of
485 Thy1+ NK cells to protective IFN- γ production during *Salmonella typhimurium* infections.
486 Proc Natl Acad Sci U S A. 2013;110(6):2252-7. Epub 2013/01/25. doi:
487 10.1073/pnas.1222047110. PubMed PMID: 23345426; PubMed Central PMCID:
488 PMC3568339.
- 489 23. Klose CS, Kiss EA, Schwierzeck V, Ebert K, Hoyler T, d'Hargues Y, et al. A T-bet
490 gradient controls the fate and function of CCR6-ROR γ t+ innate lymphoid cells. Nature.
491 2013;494(7436):261-5. Epub 2013/01/22. doi: 10.1038/nature11813. PubMed PMID:
492 23334414.
- 493 24. Spees AM, Kingsbury DD, Wangdi T, Xavier MN, Tsolis RM, Bäumlner AJ.
494 Neutrophils Are a Source of Gamma Interferon during Acute Salmonella enterica Serovar
496 Typhimurium Colitis. Infection and Immunity. 2014;82(4):1692-7. doi: 10.1128/iai.01508-
497 13.
- 498 25. Narasaraju T, Yang E, Samy RP, Ng HH, Poh WP, Liew AA, et al. Excessive
499 neutrophils and neutrophil extracellular traps contribute to acute lung injury of influenza
500 pneumonitis. Am J Pathol. 2011;179(1):199-210. Epub 2011/06/28. doi:
501 10.1016/j.ajpath.2011.03.013. PubMed PMID: 21703402; PubMed Central PMCID:
502 PMC3123873.
- 503 26. Porto BN, Stein RT. Neutrophil Extracellular Traps in Pulmonary Diseases: Too
504 Much of a Good Thing? Frontiers in immunology. 2016;7:311-. doi:
505 10.3389/fimmu.2016.00311. PubMed PMID: 27574522.

- 506 27. Lefrançois E, Mallavia B, Zhuo H, Calfee CS, Looney MR. Maladaptive role of
507 neutrophil extracellular traps in pathogen-induced lung injury. *JCI Insight*.
508 2018;3(3):e98178. doi: 10.1172/jci.insight.98178. PubMed PMID: 29415887.
- 509 28. Pulavendran S, Prasanthi M, Ramachandran A, Grant R, Snider TA, Chow VTK, et
510 al. Production of Neutrophil Extracellular Traps Contributes to the Pathogenesis of
511 *Francisella tularemia*. *Frontiers in Immunology*. 2020;11(679). doi:
512 10.3389/fimmu.2020.00679.
- 513 29. von Brühl ML, Stark K, Steinhart A, Chandraratne S, Konrad I, Lorenz M, et al.
514 Monocytes, neutrophils, and platelets cooperate to initiate and propagate venous
515 thrombosis in mice in vivo. *J Exp Med*. 2012;209(4):819-35. Epub 2012/03/28. doi:
516 10.1084/jem.20112322. PubMed PMID: 22451716; PubMed Central PMCID:
517 PMCPMC3328366.
- 518 30. Bertin F-R, Rys RN, Mathieu C, Laurance S, Lemarié CA, Blostein MD. Natural killer
519 cells induce neutrophil extracellular trap formation in venous thrombosis. *Journal of*
520 *Thrombosis and Haemostasis*. 2019;17(2):403-14. doi: 10.1111/jth.14339.
- 521 31. Xiong H, Carter RA, Leiner IM, Tang Y-W, Chen L, Kreiswirth BN, et al. Distinct
522 Contributions of Neutrophils and CCR2+ Monocytes to Pulmonary Clearance of
523 Different *Klebsiella pneumoniae* Strains. *Infection and Immunity*. 2015;83(9):3418-27.
524 doi: 10.1128/iai.00678-15. PubMed PMID: pub.1032709186.
- 525 32. Chikano S, Sawada K, Ohnishi K, Fukunaga K, Tanaka J, Shimoyama T. Interstitial
526 Pneumonia Accompanying Ulcerative Colitis. *Internal Medicine*. 2001;40(9):883-6. doi:
527 10.2169/internalmedicine.40.883.
- 528 33. Kelly MG, Frizelle FA, Thornley PT, Beckert L, Epton M, Lynch AC. Inflammatory
529 bowel disease and the lung: is there a link between surgery and bronchiectasis?
530 *International Journal of Colorectal Disease*. 2006;21(8):754-7. doi: 10.1007/s00384-
531 006-0094-9.
- 532 34. Raj AA, Birring SS, Green R, Grant A, De Caestecker J, Pavord ID. Prevalence of
533 inflammatory bowel disease in patients with airways disease. *Respiratory Medicine*.
534 2008;102(5):780-5. doi: 10.1016/j.rmed.2007.08.014.

- 535 35. Rojo ÓP, Román ALS, Arbizu EA, De La Hera Martínez A, Sevillano ER, Martínez
536 AA. Serum lipopolysaccharide-binding protein in endotoxemic patients with
537 inflammatory bowel disease. 2007;13(3):269-77. doi: 10.1002/ibd.20019.
- 538 36. Scaldaferri F, Vetrano S, Sans M, Arena V, Straface G, Stigliano E, et al. VEGF-A
539 Links Angiogenesis and Inflammation in Inflammatory Bowel Disease Pathogenesis.
540 2009;136(2):585-95.e5. doi: 10.1053/j.gastro.2008.09.064.
- 541 37. Margraf A, Ley K, Zarbock A. Neutrophil Recruitment: From Model Systems to
542 Tissue-Specific Patterns. Trends in Immunology. 2019. doi: 10.1016/j.it.2019.04.010.
- 543 38. Khajah M, Millen B, Cara DC, Waterhouse C, McCafferty DM. Granulocyte-
544 macrophage colony-stimulating factor (GM-CSF): a chemoattractive agent for murine
545 leukocytes in vivo. J Leukoc Biol. 2011;89(6):945-53. Epub 2011/03/12. doi:
546 10.1189/jlb.0809546. PubMed PMID: 21393420.
- 547 39. Laan M, Prause O, Miyamoto M, Sjostrand M, Hytonen AM, Kaneko T, et al. A role
548 of GM-CSF in the accumulation of neutrophils in the airways caused by IL-17 and TNF-
549 alpha. Eur Respir J. 2003;21(3):387-93. Epub 2003/03/29. PubMed PMID: 12661990.
- 550 40. Herold S, Hoegner K, Vadasz I, Gessler T, Wilhelm J, Mayer K, et al. Inhaled
551 granulocyte/macrophage colony-stimulating factor as treatment of pneumonia-
552 associated acute respiratory distress syndrome. Am J Respir Crit Care Med.
553 2014;189(5):609-11. Epub 2014/03/04. doi: 10.1164/rccm.201311-2041LE. PubMed
554 PMID: 24579839.
- 555 41. Quinton LJ. GM-CSF: a double dose of protection during pneumonia. Am J Physiol
556 Lung Cell Mol Physiol. 2012;302(5):L445-6. Epub 2012/01/24. doi:
557 10.1152/ajplung.00022.2012. PubMed PMID: 22268117.
- 558 42. Cheng OZ, Palaniyar N. NET balancing: a problem in inflammatory lung diseases.
559 Frontiers in immunology. 2013;4:1-. doi: 10.3389/fimmu.2013.00001. PubMed PMID:
560 23355837.
- 561 43. Yost CC, Schwertz H, Cody MJ, Wallace JA, Campbell RA, Vieira-de-Abreu A, et al.
562 Neonatal NET-inhibitory factor and related peptides inhibit neutrophil extracellular trap
563 formation. The Journal of clinical investigation. 2016;126(10):3783-98. Epub
564 2016/09/06. doi: 10.1172/JCI83873. PubMed PMID: 27599294.

- 565 44. Martinod K, Wagner DD. Thrombosis: tangled up in NETs. *Blood*.
566 2014;123(18):2768-76. doi: 10.1182/blood-2013-10-463646.
- 567 45. Fuchs TA, Brill A, Wagner DD. Neutrophil extracellular trap (NET) impact on deep
568 vein thrombosis. *Arterioscler Thromb Vasc Biol*. 2012;32(8):1777-83. Epub 2012/05/31.
569 doi: 10.1161/ATVBAHA.111.242859. PubMed PMID: 22652600.
- 570 46. Brinkmann V, Zychlinsky A. Beneficial suicide: why neutrophils die to make NETs.
571 *Nat Rev Microbiol*. 2007;5(8):577-82. Epub 2007/07/17. doi: 10.1038/nrmicro1710.
572 PubMed PMID: 17632569.
- 573 47. Simonian PL, Roark CL, Wehrmann F, Lanham AM, Born WK, O'Brien RL, et al. IL-
574 17A-expressing T cells are essential for bacterial clearance in a murine model of
575 hypersensitivity pneumonitis. *Journal of immunology (Baltimore, Md : 1950)*.
576 2009;182(10):6540-9. doi: 10.4049/jimmunol.0900013. PubMed PMID: 19414809.
- 577 48. Skerrett SJ, Martin TR, Chi EY, Peschon JJ, Mohler KM, Wilson CB. Role of the type
578 1 TNF receptor in lung inflammation after inhalation of endotoxin or *Pseudomonas*
579 *aeruginosa*. *Am J Physiol*. 1999;276(5):L715-27. Epub 1999/05/18. doi:
580 10.1152/ajplung.1999.276.5.L715. PubMed PMID: 10330027.
- 581 49. Kang MJ, Jang AR, Park JY, Ahn JH, Lee TS, Kim DY, et al. IL-10 Protects Mice
582 From the Lung Infection of *Acinetobacter baumannii* and Contributes to Bacterial
583 Clearance by Regulating STAT3-Mediated MARCO Expression in Macrophages. *Front*
584 *Immunol*. 2020;11:270. Epub 2020/03/11. doi: 10.3389/fimmu.2020.00270. PubMed
585 PMID: 32153580; PubMed Central PMCID: PMC7047127.
- 586 50. Moore TA, Standiford TJ. The role of cytokines in bacterial pneumonia: an
587 inflammatory balancing act. *Proc Assoc Am Physicians*. 1998;110(4):297-305. Epub
588 1998/08/01. PubMed PMID: 9686677.
- 589 51. Moore TA, Perry ML, Getsoian AG, Newstead MW, Standiford TJ. Divergent role of
590 gamma interferon in a murine model of pulmonary versus systemic *Klebsiella*
591 *pneumoniae* infection. *Infection and immunity*. 2002;70(11):6310-8. doi:
592 10.1128/iai.70.11.6310-6318.2002. PubMed PMID: 12379710.
- 593 52. Schultz MJ, Rijneveld AW, Speelman P, van Deventer SJ, van der Poll T.
594 Endogenous interferon-gamma impairs bacterial clearance from lungs during

- 595 Pseudomonas aeruginosa pneumonia. Eur Cytokine Netw. 2001;12(1):39-44. PubMed
596 PMID: 11282544.
- 597 53. Gregorio J, Meller S, Conrad C, Di Nardo A, Homey B, Lauerma A, et al.
598 Plasmacytoid dendritic cells sense skin injury and promote wound healing through type I
599 interferons. J Exp Med. 2010;207(13):2921-30. Epub 2010/12/01. doi:
600 10.1084/jem.20101102. PubMed PMID: 21115688; PubMed Central PMCID:
601 PMCPMC3005239.
- 602 54. Takagi H, Fukaya T, Eizumi K, Sato Y, Sato K, Shibazaki A, et al. Plasmacytoid
603 dendritic cells are crucial for the initiation of inflammation and T cell immunity in vivo.
604 Immunity. 2011;35(6):958-71. Epub 2011/12/20. doi: 10.1016/j.immuni.2011.10.014.
605 PubMed PMID: 22177923.
- 606 55. Serbina NV, Salazar-Mather TP, Biron CA, Kuziel WA, Pamer EG. TNF/iNOS-
607 producing dendritic cells mediate innate immune defense against bacterial infection.
608 Immunity. 2003;19(1):59-70. Epub 2003/07/23. doi: 10.1016/s1074-7613(03)00171-7.
609 PubMed PMID: 12871639.
- 610 56. Bieber K, Autenrieth SE. Dendritic cell development in infection. Molecular
611 Immunology. 2020;121:111-7. doi: <https://doi.org/10.1016/j.molimm.2020.02.015>.
- 612 57. Frevert CW, Huang S, Danaee H, Paulauskis JD, Kobzik L. Functional
613 characterization of the rat chemokine KC and its importance in neutrophil recruitment in
614 a rat model of pulmonary inflammation. J Immunol. 1995;154(1):335-44. Epub
615 1995/01/01. PubMed PMID: 7995953.
- 616 58. Greenberger MJ, Strieter RM, Kunkel SL, Danforth JM, Laichalk LL, McGillicuddy
617 DC, et al. Neutralization of macrophage inflammatory protein-2 attenuates neutrophil
618 recruitment and bacterial clearance in murine Klebsiella pneumonia. J Infect Dis.
619 1996;173(1):159-65. Epub 1996/01/01. doi: 10.1093/infdis/173.1.159. PubMed PMID:
620 8537653.
- 621 59. Tateda K, Moore TA, Newstead MW, Tsai WC, Zeng X, Deng JC, et al. Chemokine-
622 dependent neutrophil recruitment in a murine model of Legionella pneumonia: potential
623 role of neutrophils as immunoregulatory cells. Infect Immun. 2001;69(4):2017-24. Epub
624 2001/03/20. doi: 10.1128/iai.69.4.2017-2024.2001. PubMed PMID: 11254553; PubMed
625 Central PMCID: PMCPMC98125.

- 626 60. Huang Y, Mao K, Chen X, Sun MA, Kawabe T, Li W, et al. S1P-dependent
627 interorgan trafficking of group 2 innate lymphoid cells supports host defense. *Science*.
628 2018;359(6371):114-9. Epub 2018/01/06. doi: 10.1126/science.aam5809. PubMed
629 PMID: 29302015.
- 630 61. Mjösberg J, Rao A. Lung inflammation originating in the gut. *Science*.
631 2018;359(6371):36-7. doi: 10.1126/science.aar4301.
- 632 62. Huang Y, Guo L, Qiu J, Chen X, Hu-Li J, Siebenlist U, et al. IL-25-responsive,
633 lineage-negative KLRG1hi cells are multipotential 'inflammatory' type 2 innate lymphoid
634 cells. *Nature Immunology*. 2015;16(2):161-9. doi: 10.1038/ni.3078.
- 635 63. Burkholder T, Foltz C, Karlsson E, Linton CG, Smith JM. Health Evaluation of
636 Experimental Laboratory Mice. *Current Protocols in Mouse Biology*. 2012;2(2):145-65.
637 doi: 10.1002/9780470942390.mo110217.
- 638 64. Barthel M, Hapfelmeier S, Quintanilla-Martinez L, Kremer M, Rohde M, Hogardt M,
639 et al. Pretreatment of Mice with Streptomycin Provides a *Salmonella enterica* Serovar
640 Typhimurium Colitis Model That Allows Analysis of Both Pathogen and Host.
641 2003;71(5):2839-58. doi: 10.1128/iai.71.5.2839-2858.2003.
- 642 65. Yost CC, Schwertz H, Cody MJ, Wallace JA, Campbell RA, Vieira-de-Abreu A, et al.
643 Neonatal NET-inhibitory factor and related peptides inhibit neutrophil extracellular trap
644 formation. *J Clin Invest*. 2016;126(10):3783-98. Epub 2016/09/07. doi:
645 10.1172/jci83873. PubMed PMID: 27599294; PubMed Central PMCID:
646 PMC5096809.

647

648 **Supporting information**

649 **Supplemental Figure S1: No differences in body weight loss between mice with or**
650 **without *S. Typhimurium* prior infection post *K. pneumoniae* challenge .** Percent of
651 initial body weight, statistical analysis was performed by fitting a mixed-effect model
652 followed by Tukey's multiple comparisons test.

653 **Supplemental Figure S2: No neutrophil margination and necrotic clusters were**
654 **detected in mice with intestinal *S. Typhimurium* infection (S) and mice with *K.***
655 ***pneumoniae* respiratory infection (K).** Representative images (200x magnification) of
656 lung sections stained with hematoxylin/eosin. Data represents cumulative results of two
657 independent experiments (n = 2 for UI, n = 10 for S group, n = 9 for K group).

658 **Supplemental Figure S3: Pulmonary microthrombi in S and S+K treated mice.**
659 Lung sections from S and S+K mice show scattered thrombus formation in capillary-
660 sized vessels (black arrows), readily identified at the periphery of the lungs. H&E, 400x
661 magnification. Data represents cumulative results of two independent experiments (n =
662 2 for UI, n = 10 for S group, n = 9 for K group and n = 8 for S+K group).

663 **Supplemental Figure S4: Lung cytokine profiles showing no differences between**
664 **the groups tested.** Levels of lung inflammatory cytokines (A) IL-23, (B) IL-1 α , (C) TNF-
665 α , (D) IL-12p70, (E) IL-10, (F) IL-6, (G) IL-27, (H) IL-17A, (I) IFN β were assessed 18
666 hours post *K. pneumoniae* challenge via bead-based LEGENDplex mouse inflammation
667 panel 13-plex assay. Data represents one experiment for uninfected mice (n =6) and *S.*
668 *Typhimurium* infected mice (n =6) and cumulative results of three independent
669 experiments for K (n = 18) and S+K group (n = 19). Error bars represents mean \pm SD
670 and significance was determined by Mann-Whitney tests.

671 **Supplementary Figure S5: Mice with prior intestinal infection have lower number**
672 **of total neutrophils in lungs post intranasal challenge with *K. pneumoniae*.** Using
673 flow cytometry, total numbers of (A) neutrophils, (B) lung plasmacytoid dendritic cells
674 (pDCs) and (C) monocytic dendritic cells (moDCs), (D) CD103+ DCs, (E) alveolar
675 macrophages (AMs) and (F) interstitial macrophages (IMs) were evaluated between
676 uninfected mice (UI), *S. Typhimurium* infected mice (S), *K. pneumoniae* infected mice
677 (K) and both *S. Typhimurium* and *K. pneumoniae* infected mice (S+K). Data represents
678 cumulative results of five independent experiments (n = 22 for UI, n = 24 for S, n = 25
679 for K and n = 22 for S+K). Error bars represents mean \pm SD and significance was
680 determined by Mann-Whitney tests.

681 **Supplemental Figure S6: Mice with prior *S. Typhimurium* intestinal infection have**
682 **no differences in α NKT, MAIT and TCR $\gamma\delta$ cells in response to respiratory *K.***
683 ***pneumoniae* infection.** Using flow cytometry, percentage frequencies of (A) α NKT cells,
684 (B) MAIT cells and (C) TCR $\gamma\delta$ cells were evaluated between uninfected mice (UI), *S.*
685 *Typhimurium* infected mice (S), *K. pneumoniae* infected mice (K) and both *S.*
686 *Typhimurium* and *K. pneumoniae* infected mice (S+K). Data represents cumulative
687 results of five independent experiments (n = 22 for UI, n = 24 for S, n = 25 for K and n =
688 22 for S+K). Error bars represents mean \pm SD and statistical significance was
689 determined by using Mann-Whitney tests.

690 **Supplemental Figure S7: Mice with prior *S. Typhimurium* intestinal infection have**
691 **no differences in blood leukocytes and platelets in response to respiratory *K.***
692 ***pneumoniae* infection.** Using Hemavet analyzer, percentage frequencies of (A)
693 neutrophils, (B) lymphocytes, (C) monocytes, (D) eosinophils, (E) basophils and blood
694 platelet counts were assessed between *K. pneumoniae* infected mice (K) and both *S.*
695 *Typhimurium* and *K. pneumoniae* infected mice (S+K). Data represents results of one
696 experiment (n = 4 for K and n = 4 for S+K). Error bars represents mean \pm SD and
697 statistical significance was determined by using Mann-Whitney tests. Data were
698 analyzed by t-test and presented in mean \pm SD.

Fig 1

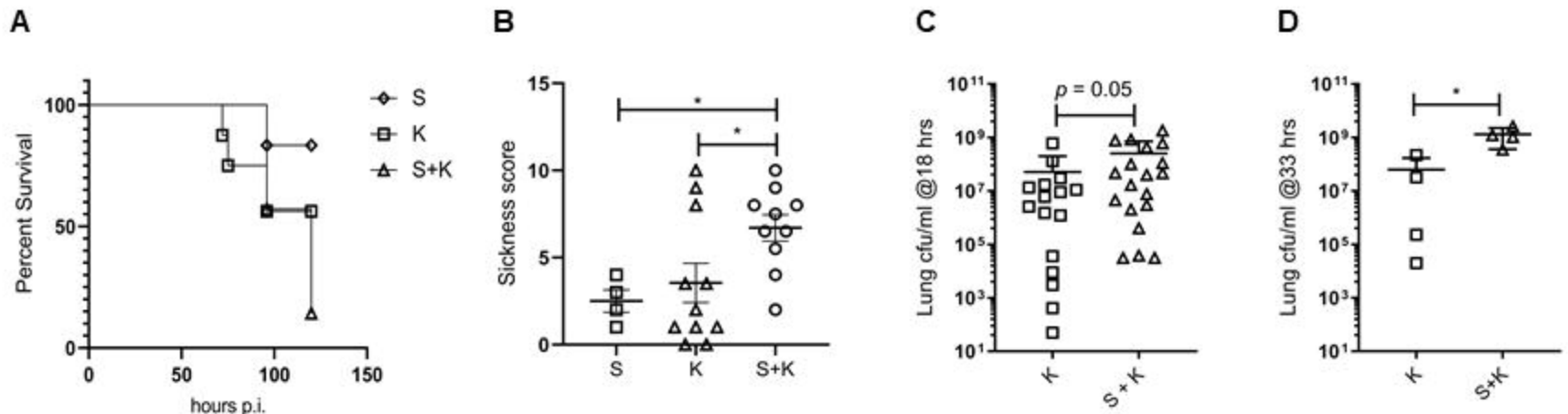
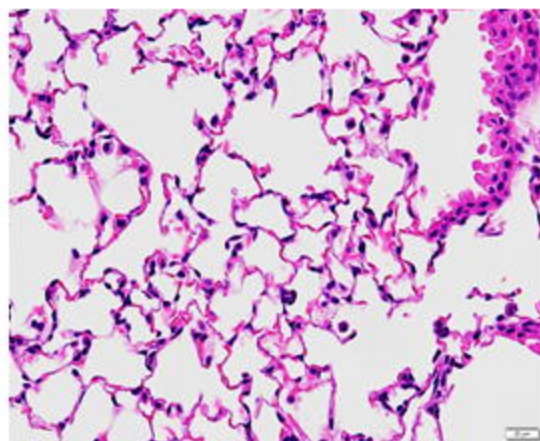


Fig 1: Mice with prior *S. Typhimurium* intestinal infection have increased susceptibility to respiratory *K. pneumoniae* infection. (A) Kaplan-Meier survival curves of mice infected with *S. Typhimurium* intestinal infection (S), *K. pneumoniae* infection only (K) and mice with prior *S. Typhimurium* intestinal infection and challenged with *K. pneumoniae* infection (S+K). Statistical analysis was performed using log-rank (Mantel-Cox) test, $p = 0.07$ and log-rank test for significant trend, $p = 0.02$ (B) sickness score plots where data represents cumulative results of two independent experiments ($n = 4-6$ for S, $n = 11$ for K and $n = 10$ for S+K) and mean \pm SD, * denotes $p < 0.05$. Statistical analysis was performed using Kruskal-Wallis test followed by Dunn's multiple comparison test. (C) *K. pneumoniae* bacterial load determined in lungs at 18 hours post *K. pneumoniae* infection in both K and S+K groups. Data represents cumulative results of three independent experiments ($n = 16$ for K and $n = 19$ for S+K). (D) Lung bacterial loads also determined at 33 hours in both groups ($n = 4$ for each group). For (C) and (D) data represents mean \pm SD and statistical analysis was determined using Mann-Whitney test, * denotes $p < 0.05$.

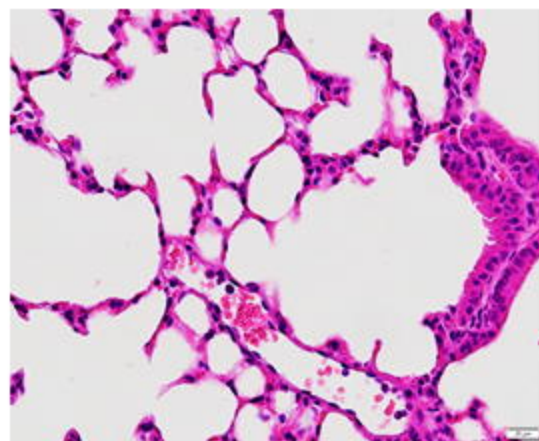
Fig 2

A

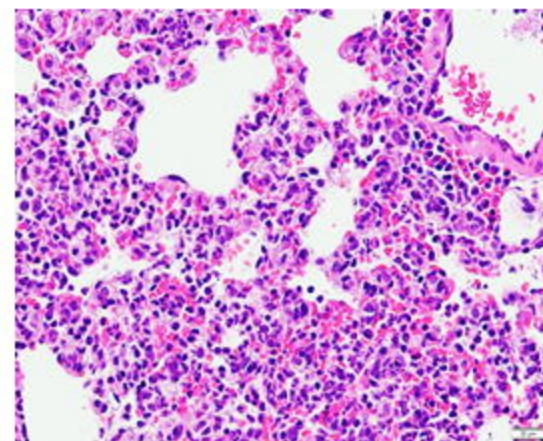
Uninfected



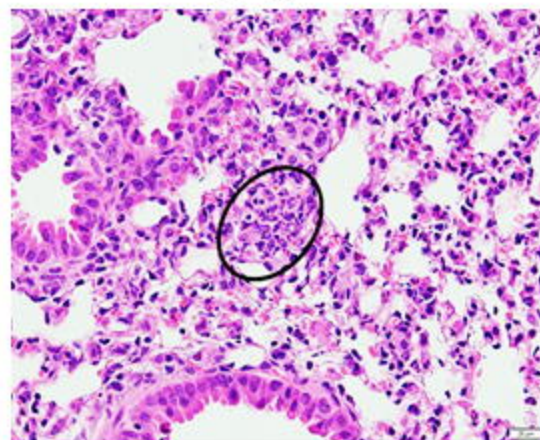
S



K



S+K



S+K

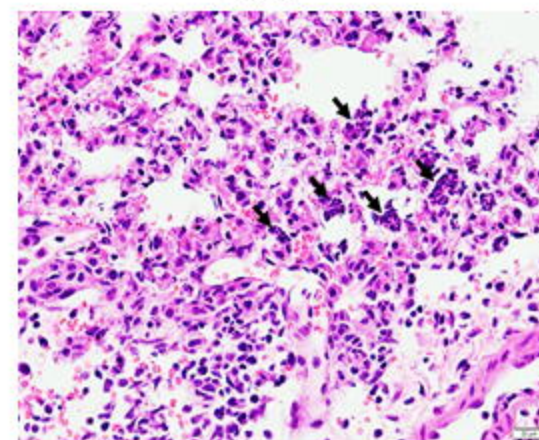


Fig 2

B

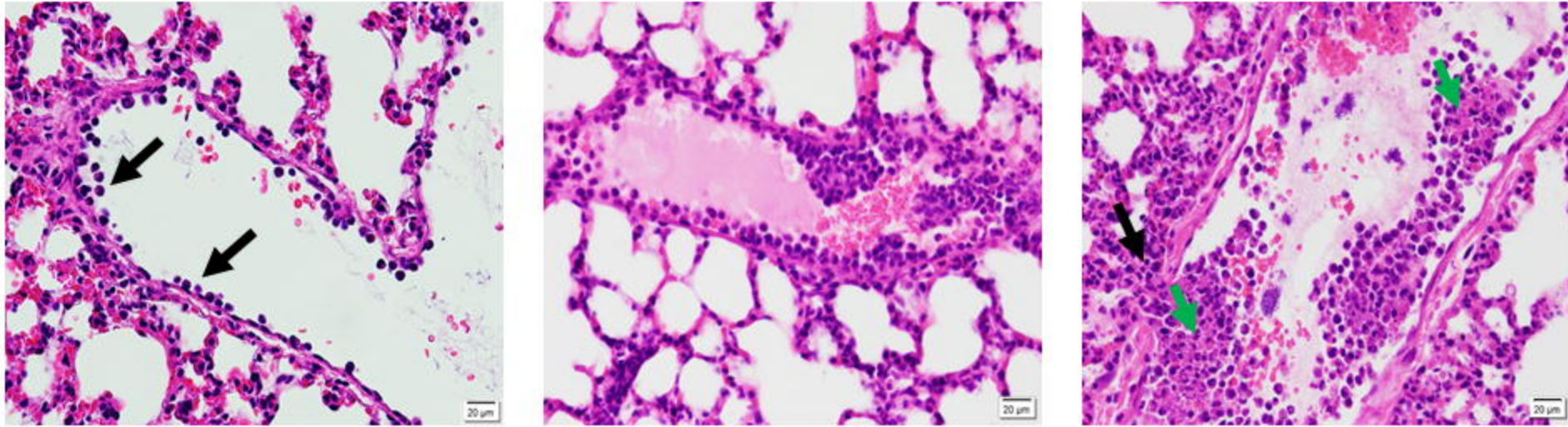


Fig 2: Mice with prior *S. Typhimurium* intestinal infection have increased lung inflammation from subsequent respiratory *K. pneumoniae* infection, characterized by microabscess, pyknotic neutrophils and margination, compared to those with no prior intestinal infection. (A) Representative images (400x magnification, scale bar = 20 µm) of lung sections stained with hematoxylin/eosin, normal lung in uninfected mice and in mice with intestinal infection (S). K mice show mixed interstitial inflammatory consolidations. Microabscess (circled) and clusters of pyknotic neutrophils (arrows) are apparent in mice with prior intestinal *S. Typhimurium* infection and challenged with *K. pneumoniae* infection (S+K). (B) Representative images (H & E, 400x magnification, scale bar = 20 µm) of lung sections of S + K infected mice. Lung vessels in S + K infected mice showing neutrophil margination (left, black arrows), margination and clustering (middle), necrotic clusters (right, green arrow) and extravasation (right, black arrow). Data represents cumulative results of two independent experiments (n = 2 for UI, n = 10 for S group, n = 9 for K group and n = 8 for S+K group).

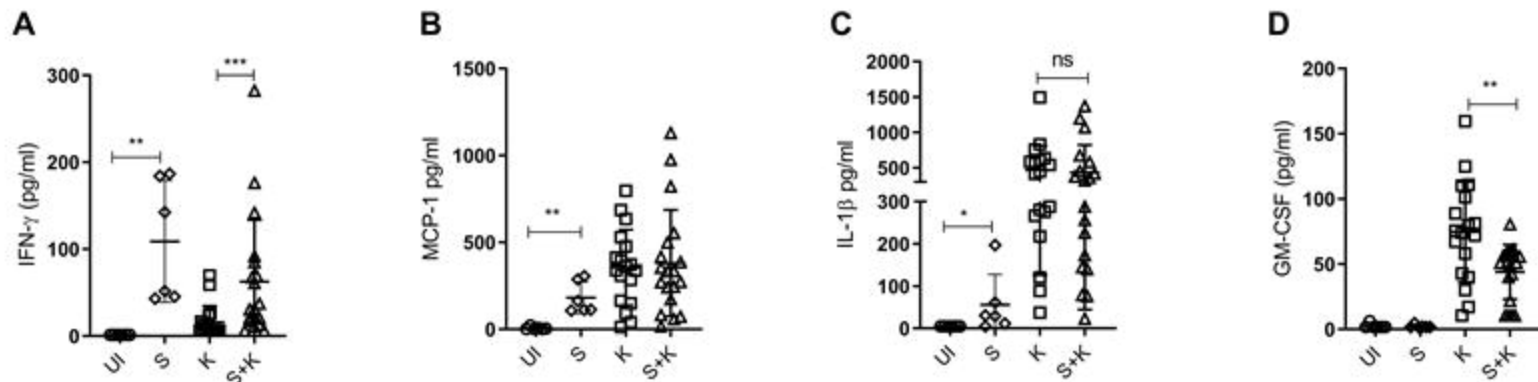
Fig 3

Fig 3: Mice with prior *S. Typhimurium* intestinal infection have altered lung cytokine profiles, and altered cytokine responses to respiratory *K. pneumoniae* infection, compared to those with no prior intestinal infection. Levels of lung inflammatory cytokines (A) IFN- γ , (B) MCP-1, (C) IL-1 β and (D) GM-CSF were assessed 18 hours post *K. pneumoniae* challenge via bead-based LEGENDplex mouse inflammation panel 13-plex assay. Data represents one experiment for uninfected mice (n =6) and *S. Typhimurium* infected mice (n =6) and cumulative results of three independent experiments for K (n = 18) and S+K group (n = 19). Error bars represents mean \pm SD and significance was determined by Mann-Whitney tests.

Fig 4

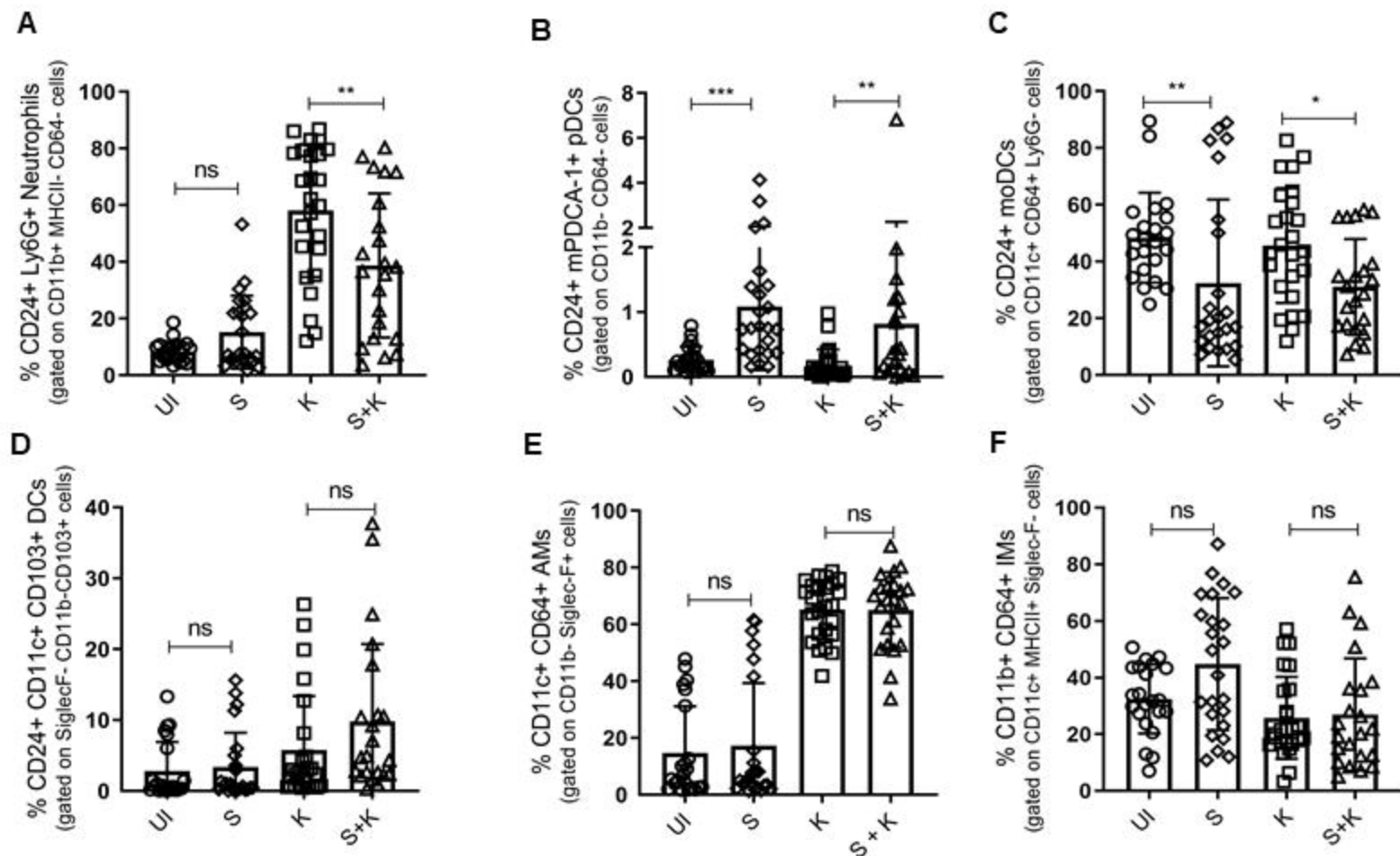


Fig 4: Mice with prior *S. Typhimurium* intestinal infection have altered frequencies of innate cell types in the lung, and altered lung innate cellular responses to respiratory *K. pneumoniae* infection. Using flow cytometry, percentage frequencies of (A) neutrophils, (B) lung plasmacytoid dendritic cells (pDCs), (C) monocytic dendritic cells (moDCs), (D) CD103+ DCs, (E) alveolar macrophages (AMs) and (F) interstitial macrophages (IMs) were evaluated between uninfected mice (UI), *S. Typhimurium* infected mice (S), *K. pneumoniae* infected mice (K) and both *S. Typhimurium* and *K. pneumoniae* infected mice (S+K). Data represents cumulative results of five independent experiments (n = 22 for UI, n = 24 for S, n = 25 for K and n = 22 for S+K). Error bars represents mean \pm SD and statistical significance was determined by using Mann-Whitney tests.

Fig 5

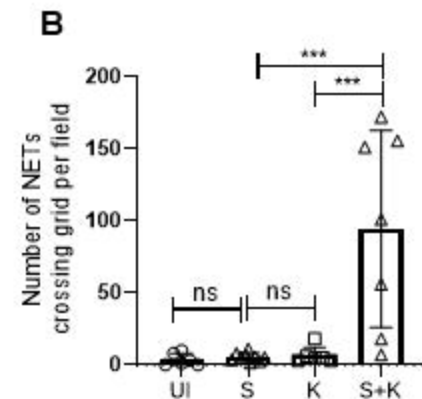
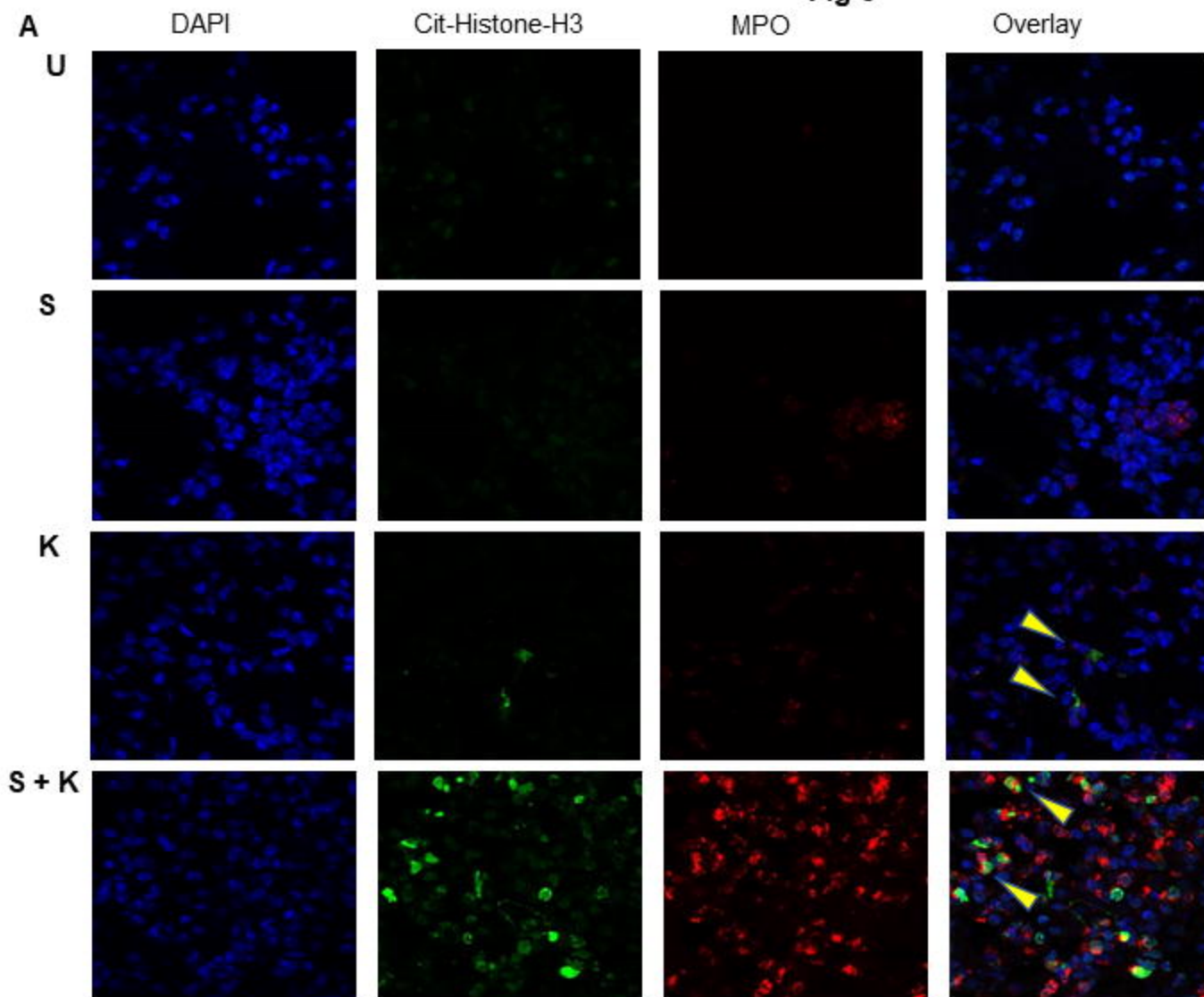


Fig 5: Mice with prior *S. Typhimurium* intestinal infection have increased NETosis in lungs from subsequent respiratory *K. pneumoniae* infection, compared to those with no prior intestinal infection. (A) Using Olympus FV3000 Confocal Laser Scanning Microscope, NET formation was assessed in all four groups and images were taken at 60X magnification. Blue fluorescence, nuclear DNA; green fluorescence, NET-associated citrullinated histone H3; red fluorescence, myeloperoxidase (MPO); NETs, yellow arrows in overlay. (B) Bar graph showing number of NETs crossing grid per field. One-way ANOVA with Tukey's post hoc testing. *** denotes $P < 0.001$.